Structural and Dynamical Properties of the Hg 2+ Aqua Ion: A Molecular Dynamics Study

ARTICLE *in* THE JOURNAL OF PHYSICAL CHEMISTRY B · MAY 2008

Impact Factor: 3.3 · DOI: 10.1021/jp074545s · Source: PubMed

Structural and Dynamical Properties of the Hg^{2+} Aqua Ion: A Molecular Dynamics Study

Giordano Mancini,[†,‡] Nico Sanna,[†] Vincenzo Barone,[§] Valentina Migliorati,[‡] Paola D'Angelo,*[,‡] and Giovanni Chillemi*[,†]

CASPUR, Consortium for Supercomputing Applications, Via dei Tizii 6b, 00185 Rome, Italy, Department of Chemistry, University of Rome "La Sapienza", Piazzale Aldo Moro 5, 00185 Rome, Italy, and Department of Chemistry, University of Naples Federico II, Via Cintia, 80126 Naples, Italy

Received: June 12, 2007; In Final Form: January 13, 2008

Molecular dynamics simulations of the Hg^{2+} ion in aqueous solution have been carried out using an effective two-body potential derived from quantum mechanical calculations. A stable heptacoordinated structure of the Hg^{2+} first hydration shell has been observed and confirmed by extended X-ray absorption fine structure (EXAFS) experimental data. The structural properties of the Hg^{2+} hydration shells have been investigated using radial and angular distribution functions, while the dynamical behavior has been discussed in terms of reorientational correlation functions, mean residence times of water molecules in the first and second hydration shells, and self-diffusion coefficients. The effect of water−water interactions on the Hg^{2+} hydration properties has been evaluated using the SPC/E and TIP5P water models.

1. Introduction

Knowledge of the structural and dynamic properties of the hydration sphere of aqua ions is fundamental to understanding the behavior of ions in chemical and biological systems. While a considerable amount of work has been devoted to characterize the hydration complexes of 3d transition-metal ions, the solution structure of the Hg^{2+} aqua ion has been poorly defined because of the lack of experimental techniques able to provide reliable information.[1]

The Hg^{2+} ion has usually been described as being octahedrally coordinated by water,[2] similarly to other transition metal ions such as Zn^{2+}, Co^{2+}, and Ni^{2+},[3] although a degree of uncertainty has been caused by the variety of coordination structures found in solid complexes,[1] and by the quite short mean residence time of water molecules in the first coordination shell (on the order of 1 ns)[4] as compared to divalent first-row transition ions, indicating a larger flexibility of the Hg^{2+} hydration complex. Moreover, the radial distribution function obtained from X-ray diffraction (XRD) shows an unexpectedly large variation in the Hg−O bond lengths, explained by a pseudo Jahn−Teller effect in the octahedral complex.[5]

Recently, the Hg^{2+} hydration structure has been studied by neutron diffraction (ND) with isotopic substitution.[6] The conclusion drawn by the authors is that the first solvation shell contains six water molecules, even though the actual experimental determination of the number of D atoms around the Hg^{2+} ion is 13.5 ± 2.1, thus suggesting a higher coordination number.

From a computational point of view, several approaches have been used to investigate the properties of the Hg^{2+} aqua ion. These include quantum mechanical *ab initio* calculations on $Hg^{2+}-(H_2O)_n$ clusters,[5] classical molecular dynamics (MD) simulations (both with simple pair potentials and including three-body corrections),[7] and *ab initio* quantum mechanics/molecular mechanics (QM/MM)[8,9] simulations, all describing the Hg^{2+} innermost hydration shell as an octahedral complex. Quantum mechanical Car−Parrinello or QM/MM simulations are computationally very expensive, and can be used only in short simulations (up to a few tens or a few hundreds of picoseconds), and thus they can be affected by poor sampling if used to investigate transport properties occurring on the nanosecond or longer time scale. On the other hand, classical MD can be used to obtain simulations several orders of magnitude longer, but the proper choice of the interaction potentials used is always a mandatory prerequisite for a reliable description of the system under investigation.[10−12]

Recently, we have developed an effective two-body potential that has been used in classical MD simulations of Hg^{2+} in aqueous solution.[13] Using a combined experimental and computational approach, we have shown that, at variance with all the reported results, the Hg^{2+} ion in aqueous solution forms a quite flexible heptacoordinated first hydration shell complex. In light of the recent experimental ND results, interpreted once more in terms of a hexacoordinated hydration complex for the Hg^{2+} ion,[6] we have decided to provide a definite answer to this controversial issue. To this end, we have carried out thorough MD investigations using different potentials and water models, and we have derived accurate structural and dynamic properties of the Hg^{2+} first and second hydration shells. The theoretical structural results have been compared with extended X-ray absorption fine structure (EXAFS) experimental data. The combination of MD simulations and EXAFS spectroscopy is a well-known performing technique to unravel the structure of electrolytic solutions, especially for metal cations in a disordered environment. Moreover, the use of two of the most widespread water models, namely the SPC/E[14] and TIP5P,[15] allowed us to assess how water−water interactions influence the structural and dynamic properties of the Hg^{2+} hydration shells obtained from MD simulations.

2. Methods

2.1. Molecular Dynamics Simulations. The MD simulations of the Hg^{2+} ion in aqueous solution have been performed using

* Corresponding author.
† CASPUR.
‡ University of Rome "La Sapienza".
§ University of Naples Federico II.

10.1021/jp074545s CCC: $40.75
Published on Web 03/27/2008

TABLE 1: Estimated $Hg^{2+}-H_2O$ Interaction Parameters with Their Relative Standard Deviations for the TIP5P Water Model

$Hg^{2+}-O$ parameters (std. dev.)		$Hg^{2+}-H,-L$ parameters (std. dev.)	
A_O	$0.3718\ (6.40 \times 10^{-2})$	A_H	$1.169 \times 10^{-1}\ (1.85 \times 10^{-3})$
B_O	$0.7620 \times 10^{-1}\ (4.05 \times 10^{-3})$	B_H	$-6.900 \times 10^{-4}\ (4.10 \times 10^{-5})$
C_O	$-1.021 \times 10^{-3}\ (5.52 \times 10^{-5})$	C_H	$1.606 \times 10^{-6}\ (8.87 \times 10^{-8})$
D_O	$4.493 \times 10^{-8}\ (2.54 \times 10^{-9})$	A_L	$1.208 \times 10^{-1}\ (5.18 \times 10^{-3})$
E_O	$-6.681 \times 10^{5}\ (3.97 \times 10^{3})$	B_L	$-1.590 \times 10^{-3}\ (1.07 \times 10^{-4})$
F_O	$2.015 \times 10^{1}\ (2.25 \times 10^{-1})$	C_L	$6.729 \times 10^{-6}\ (6.27 \times 10^{-7})$

effective two-body potentials obtained by fitting the parameters of a suitable analytical function on an *ab initio* potential energy surface (PES). The *ab initio* PES was generated taking into account scalar relativistic effects using a suitable effective core potential and including many-body effects by means of a procedure already employed for other aqua ions.[3,13] We recall that inclusion of explicit many-body effects is crucial for the description of ions in aqueous solution and that our approach accounts for averaged many-body terms in an effective two-body classical potential.[13] We have previously shown that the pure pair additive potential is more attractive and gives rise to a longer Hg−O coordination distance as compared to the effective two-body one. All the details about the generation of the potential energy function used in the MD simulation can be found in ref 13. Both the SPC/E and the TIP5P water models have been employed in the simulations. The SPC/E is a water model with an OH distance of 1 Å and a A(HOH) angle of 109.47°, while the oxygen and hydrogen charges are −0.8476 and 0.4238 a.u., respectively. The TIP5P water model has the experimental geometry[16] (OH distance of 0.9575 Å and A(HOH) angle of 104.51°), with atomic charges of 0, 0.4238, and −0.4238 a.u. for the O, H, and L atoms, respectively (where L are two massless dummy atoms placed orthogonal to the water plane). For the TIP5P water model, we have used the following $Hg^{2+}-H_2O$ potential energy function:

$$U(r) = \frac{A_O}{r_{io}^{4}} + \frac{B_O}{r_{io}^{6}} + \frac{C_O}{r_{io}^{8}} + \frac{D_O}{r_{io}^{12}} + E_O e^{-F_O r_{io}} + \sum_{ih=ih1,ih2} \frac{q_i q_h}{r_{ih}} + \frac{A_H}{r_{ih}^{4}} + \frac{B_H}{r_{ih}^{6}} + \frac{C_H}{r_{ih}^{8}} + \sum_{iL=iL1,iL2} \frac{q_i q_L}{r_{iL}} + \frac{A_L}{r_{iL}^{4}} + \frac{B_L}{r_{iL}^{6}} + \frac{C_L}{r_{iL}^{8}} \quad (1)$$

where r_{io}, r_{ih}, and r_{iL} are the Hg−oxygen, Hg−hydrogen, and Hg-dummy atom distances, respectively, while q_i, q_h, and q_L are the atomic charges of the Hg, H, and dummy atoms, respectively; the A_O-F_O, A_H-C_H, and A_L-C_L parameters are reported in Table 1. A different potential energy function has been used for the SPC/E water model, and all details are reported in ref 13.

The simulations were carried out using the GROMACS package, version 3.2.1[17] modified in order to include the two effective pair potentials. The system was composed by one Hg^{2+} ion and 819 water molecules in a cubic box, using periodic boundary conditions. The system has been simulated in an NVT ensemble, where the temperature was kept fixed at 300 K using the Berendsen method[18] and with a coupling constant of 0.1 ps. A cutoff of 9 Å was used to deal with nonbonded interactions, with the particle mesh Ewald method to treat long-range electrostatic effects.[19,20] A homogeneous background charge has been used to compensate for the presence of the Hg^{2+} ion.[21] The simulations were carried out for 65 ns, with a time step of 1 fs, saving a configuration every 25 time steps. In both simulations, the first 5 ns have been used to equilibrate the system and are not employed in the subsequent sampling.

2.2. Structural Analysis. The structural properties of the Hg^{2+} ion are described in terms of radial distribution functions,[22] $g_{Hg-O}(r)$ and $g_{Hg-H}(r)$:

$$g_{AB}(r) = \frac{\langle \rho_B(r) \rangle}{\langle \rho_B \rangle_{local}} = \frac{1}{N_A \langle \rho_B \rangle_{local}} \sum_{i \in A}^{N_A} \sum_{j \in B}^{N_B} \frac{\delta(r_{ij} - r)}{4\pi r^2} \quad (2)$$

where $\langle \rho_B(r) \rangle$ is the particle density of type B at distance r around type A, and $\langle \rho_B \rangle_{local}$ is the particle density of type B averaged over all spheres around particles A.

To describe the distribution of water molecules around the Hg^{2+}, axial-radial 2D density maps have been calculated. These maps show the average density of water oxygen atoms in a plane perpendicular to the chosen reference axis, containing the ion and the oxygen atom of a chosen water molecule. Axial−radial density maps are particularly useful to put in evidence if, on the average, the first shell water molecules remain in a fixed position or move and exchange their positions around the ion.

Angular distribution functions have been calculated for three different angles: the one formed by the water molecular dipole vector and the Hg−O vector directions (called tilt angle and labeled as ψ), the angle formed by two different Hg−O vectors in the first shell (labeled as φ), and the dihedral angle (labeled as ζ) formed by the Hg−O−H1 plane and the Hg−O−H2 plane, where H1 and H2 are the two hydrogen atoms in the same water molecule. The radial and angular distribution functions have been obtained using in-house written codes, while 2D density maps have been generated using a standard GROMACS analysis tool (g_densmap).[23]

2.3. Dynamic Analysis. The Hg^{2+} diffusion coefficient, D_{Hg}, has been calculated from the mean square displacement using the Einstein relation:[22]

$$6D_{Hg} = \lim_{t \to \infty} \langle ||\mathbf{r}_{Hg}(t) - \mathbf{r}_{Hg}(0)|| \rangle \quad (3)$$

where $\mathbf{r}_{Hg}(0)$ is the Hg^{2+} initial position and $\mathbf{r}_{Hg}(t)$ is the position of the ion at time t.

A detailed view of the dynamics of water molecules around the Hg^{2+} ion can be obtained using the reorientational correlation function, defined as

$$C_l^{\alpha}(t) = \langle P_l(\mathbf{u}^{\alpha}(t) \cdot \mathbf{u}^{\alpha}(0)) \rangle \quad (4)$$

where P_l is the lth rank Legendre polynomial, and $\mathbf{u}^{\alpha}$ is an unit vector in a certain direction at time t. By fitting $C_l^{\alpha}(t)$ to an exponential function, $C_l^{\alpha}(t) = e^{-t/\tau l}$, it is possible to determine the correlation time, τ_l, defined as the rotation time of the $\mathbf{u}^{\alpha}$ vector. For our analysis, we used $l = 1$ and three different directions: the normal to the water molecular plane passing through the center of the oxygen atom $\mathbf{u}^{\mathbf{N}}$, a vector along the H−H direction $\mathbf{u}^{\mathbf{HH}}$, and the molecular dipole moment vector $\mathbf{u}^{\mathbf{D}}$ (see inset in Figure 6B for a definitions of these vectors); $\mathbf{u}^{\mathbf{D}}$ is correlated to the dielectric relaxation rates, while $\mathbf{u}^{\mathbf{HH}}$ is correlated to 1H−1H NMR dipolar relaxation experiments.[24] Using an approach already implemented for pure water,[25] we

have employed a mixed integration−exponential fit method to evaluate the first rank correlation times, thus minimizing the noise introduced by slow convergence of the correlation function tail. Direct integration was used in the initial part of the function, while the tail contribution was taken into account with an exponential fit. Because of the different behavior of first-shell correlation functions, caused by the presence of the Hg^{2+} ion, we have used different time windows for direct integration: a value of 15 ps has been used for $\mathbf{u}^{\mathbf{D}}$, while the $\mathbf{u}^{\mathbf{N}}$ and $\mathbf{u}^{\mathbf{HH}}$ correlation functions were explicitly integrated up to 5 ps. For bulk water, the switch value was always 5 ps.

The mean residence time of water molecules in the first hydration shell has been evaluated using two different methods. The approach proposed by Impey et al.[26] is based on the definition of a survival probability function $P_j(t, t_n, t^*)$, which takes the value one if the water molecule j lies within the referred hydration shell at both time steps t_n and $t + t_n$ and does not leave the coordination shell for any continuous period longer than t^*, otherwise it is zero. From P_j it is possible to evaluate the time-dependent coordination number (or survival function) $n_{hyd}(t)$:

$$n_{hyd}(t) = \frac{1}{N_t}\sum_{n=1}^{N_t}\sum_{j} P_j(t_n,t,t^*) \qquad (5)$$

where N_t is the total number of steps, and the summation goes over all water molecules. At long times, $n_{hyd}(t)$ decays in an exponential fashion, with a characteristic correlation time τ_{lm}, which defines the residence time of the water molecule in the shell.

A second approach, called the "direct method" and proposed by Rode et al.,[27] calculates the water residence time τ_{dir} as

$$\tau_{dir} = \frac{t_{sim}\cdot n_{hyd}(0)}{N_{ex}} \qquad (6)$$

where t_{sim} is the total simulation time, $n_{hyd}(0)$ is the average coordination number, and N_{ex} is the number of solvent exchanges between the hydration shell and the rest of the solvent; to be considered an event, such a solvent exchange event (involving a water molecule either entering or leaving the hydration shell under investigation) has to last more than the chosen t^*, which has the same role as in the Impey procedure.

The mean square displacement and diffusion coefficients have been calculated using the program g_msd from the GROMACS package.[23] A slightly modified version of a standard GROMACS tool (g_rotacf) has been used to calculate the reorientational correlation functions, while in-house written codes have been employed for water residence time.

2.4. EXAFS Data Analysis. A 0.1 M Hg^{2+} water solution was obtained by dissolving the appropriate amount of hydrated $Hg(ClO_4)_2\cdot 3H_2O$ in freshly distilled water that was acified to about pH = 1 by adding $HClO_4$ in order to prevent hydrolysis. Hg L_{III} XAS spectra were obtained at the X-ray absorption spectrometer BM29[28] of the European Synchrotron Radiation Facility (ESRF). Spectra were recorded in transmission mode using a Si(311) double-crystal monochromator detuned to 50%. Data points were collected for 1 s each, and three spectra were recorded and averaged. The solution was kept in a cell with Kapton film windows and Teflon spacers of 4 mm.

The relation between the EXAFS $\chi(k)$ signal and the local structure, defined through the n-body distribution functions, contains the integrals of the two-atom ($\gamma^{(2)}$), three-atom ($\gamma^{(3)}$) and n-atom ($\gamma^{(n)}$) signals, which can be calculated using the multiple-scattering (MS) theory.[29] In the EXAFS data analysis of disordered systems, only two-body distributions are usually considered, and the $\chi(k)$ signal is represented by the equation

$$\chi(k) = \int_0^\infty \mathrm{d}r 4\pi\rho r^2 g(r) A(k,r)\sin[2kr + \phi(k,r)] \qquad (7)$$

where $A(k,r)$ and $\phi(k,r)$ are the amplitude and phase functions, respectively, and ρ is the density of the scattering atoms. $\chi(k)$ theoretical signals can be calculated by introducing in eq 7 the model radial distribution functions obtained from dynamics simulations. Both the Hg−O and Hg−H $g(r)$'s obtained from the simulations have been used to calculate the single scattering first-shell $\chi(k)$ theoretical signal. Moreover, we have calculated the three-body contributions within the first hydration shell from the $g(r_1, r_2, \psi)$ distribution obtained from the simulations for the seven-coordinated cluster. The MS contributions within the first hydration shell have been found to have negligible amplitude, and therefore they have not been considered in the analysis of the EXAFS data. The EXAFS theoretical signals associated with all the two- and three-body distributions have been calculated by means of the GNXAS program, and a thorough description of the theoretical framework for the multiple scattering analysis can be found in ref 29. Phase shifts, $A(k,r)$ and $\phi(k,r)$, have been calculated starting from one of the MD configurations by using muffin-tin potentials and advanced models for the exchange-correlation self-energy (Hedin−Lundqvist).[30] Inelastic losses of the photoelectron in the final state have been intrinsically accounted for by complex potential. The imaginary part also includes a constant factor accounting for the core-hole width (5.50 eV).[31] As previously mentioned, the structural parameters were kept fixed during the minimization, while two nonstructural parameters were optimized: S_0^2, which accounts for an overall intensity rescaling of the amplitude, and E_0, which aligns the experimental and theoretical energy scales.

TABLE 2: Total Lifetimes, Longest Lifetimes, and Number of Solvent Exchanges between First Shell and Bulk Water for the Hexa-, Hepta-, and Octacoordinated Clusters for the TIP5P and SPC/E Simulations

	total lifetime (%)		longest lifetime (ns)		number of exchanges	
	TIP5P	SPC/E	TIP5P	SPC/E	TIP5P	SPC/E
n_{hyd}[a] = 6	4.6	2.6	1.76	0.37	15	8
n_{hyd} = 7	95.3	96.8	6.05	8.02	25	21
n_{hyd} = 8	0.1	0.6	0.02	0.14	10	13

[a] n_{hyd} is the cluster hydration number.

3. Results

3.1. Molecular Dynamics. Two MD simulations have been carried out for 65 ns, with the TIP5P and SPC/E water models. Both simulations started from a hexacoordinated first-shell configuration, and, after an induction time of 630 and 755 ps for the SPC/E and TIP5P trajectories, respectively, the system goes to heptacoordination, which remains stable for most of the simulation time. Because of the existence of such transient phenomena lasting in the nanosecond time scale, very long equilibration times (5 ns) have been used in both simulations, and the subsequent 60 ns have been used to derive structural and dynamic properties. Table 2 shows the percentages of the different hydration numbers observed in the SPC/E and TIP5P simulations, together with the number of solvent exchanges with bulk, and the longest lifetimes of each coordination complex. The 7-fold coordination is by far the most abundant for both simulations, although a small fraction of frames with $n_{hyd} = 6$

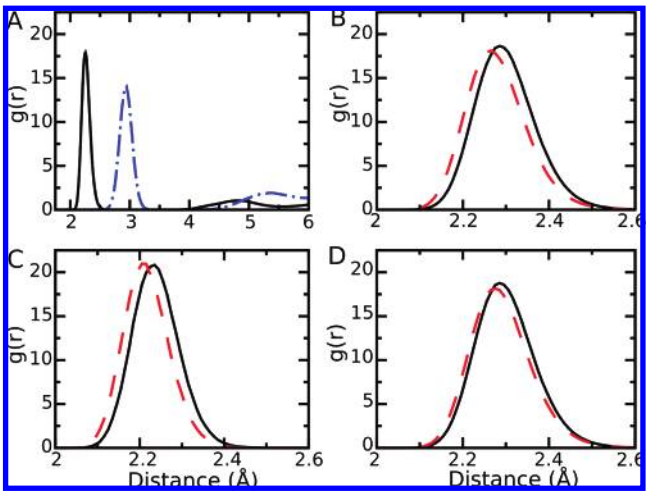

Figure 1. (A) Hg^{2+}−O radial distribution function (solid black line), and Hg^{2+}−H radial distribution function (blue dot−dashed line) for the TIP5P simulation. (B) Hg^{2+}−O radial distribution functions for the SPC/E (solid black line) and TIP5P water model (dashed red line). (C) Hg^{2+}−O radial distribution functions for the SPC/E (solid black line) and TIP5P water model (dashed red line) calculated on the six-coordinated frames. (D) Hg^{2+}−O radial distribution functions for the SPC/E (solid black line) and TIP5P water model (dashed red line) calculated on the seven-coordinated frames.

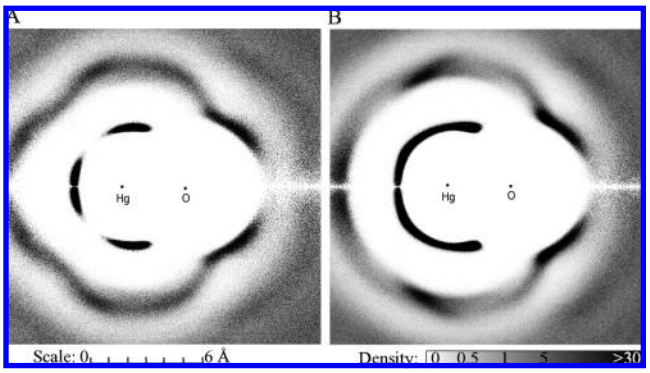

Figure 2. Axial−radial 2D density map of water molecules around a fixed Hg−O axis for the TIP5P simulation. (A) Oxygen distribution function calculated from six-coordinated frames. (B) Oxygen distribution function calculated from seven-coordinated frames.

and $n_{hyd} = 8$ is present. Both the SPC/E and TIP5P trajectories have been filtered, separating frames with six- and seven-coordinated first hydration shells, and structural properties have been calculated for these two complexes. On the other hand, frames with eight water molecules in the first shell are much less abundant, and the corresponding time windows are much shorter (up to 20 ps). For this reason the octahydrated complex has been considered as a transition structure for the solvent exchange reaction of the seven-coordinated complex. As average quantities calculated on the whole trajectory are often coincident with those obtained from the seven-coordinated trajectory, these last are reported unless otherwise noted.

3.2. Hydration Structure. The Hg−O and Hg−H radial distribution functions obtained using the TIP5P water model are shown in Figure 1A. The two $g(r)$'s have well-defined first peaks followed by a depletion zone, showing the existence of a quite stable first hydration shell. The first shell maximum of the Hg−O $g(r)$ is at 2.26 Å, and the corresponding hydrations number is 6.9 for the TIP5P simulation. The SPC/E first maximum is found at a slightly longer distance (2.28 Å) with a coordination number of 7. As far as the Hg−H $g(r)$'s are concerned, the first shell maxima are found at 2.97 and 2.94 Å for the SPC/E and TIP5P models, respectively, with coordination numbers of 13.8 and 14. Figure 1B shows the comparison between the Hg−O $g(r)$'s obtained from the SPC/E and TIP5P simulations. To better understand the origin of the small difference, it is useful to analyze the $g(r)$'s obtained from hexa- and heptacoordinated simulation frames, separately. Inspection of Figure 1C shows that the biggest difference is detected for the octahedral clusters (0.03 Å), while the seven-coordinated complexes have similar distance distribution (octahedral clusters' peak positions are at 2.23 and 2.20 Å for the SPC/E and TIP5P simulations, while heptacoordinated ones are at 2.28 and 2.27 Å). Note that the octahedral structure is present only for small percentages of the simulation time in both trajectories, and therefore it has a small effect on the position of the $g_{Hg-O}(r)$ first maxima. For the subsequent analyses, we have used a Hg−O distance of 3.2 Å as a cutoff value to distinguish between the first and second hydration shell, and a distance of 5.5 Å to separate the second hydration shell from bulk water molecules.

The flexibility of the Hg^{2+} first hydration shell can be highlighted using axial-radial 2D density projection maps for the six- and seven-coordinated complexes (see Figure 2A,B for the TIP5P simulation). Very similar results have been obtained from the two simulations, and only the analysis of the TIP5P trajectory is shown for the sake of brevity. The map in Figure 2A is typical of an octahedral cluster, such as that obtained for the Ni^{2+} hydrated ion.[12] On the contrary, in the case of the seven-coordinated structure, the oxygen atoms give rise to a uniform distribution around the selected axis (see Figure 2B), showing the higher mobility of the first-shell water molecules.

The geometrical arrangement of the first shell water molecules around the Hg^{2+} ion for the six- and seven-coordinated complexes can be evaluated by looking at the angular distribution functions of the A(OHgO) (ψ) and A(HgOH) angles (ϕ), plotted as $1 - \cos(x)$, ($x = \phi,\psi$), using a $\cos(x)$ step of 0.001°. Figure 3A shows the A(OHgO) angular distribution function for the hepta- and hexacoordinated clusters obtained from the TIP5P simulation. For the 6-fold coordinated shells, the maxima are located at $1 - \cos(\psi) = 1$ and $1 - \cos(\psi) = 2$, corresponding to ψ values of 90° and 180°, as expected for an octahedral hydration complex. The peak maxima for the 7-fold coordinated structure are found at ψ values of about ∼75° and ∼145° for both simulations. These results can be better understood by looking at the structures of the heptacoordinated complex corresponding to the QM minimum energy at the MP2 level of computation,[13] shown in Figure 3B, where the $A(O_1HgO_2)$ and $A(O_1HgO_3)$ angles are about 75° and 145°. Figure 3C shows the ϕ angular distribution functions calculated for first and second hydration shells, and bulk water for the TIP5P simulation. The most probable value of ϕ for the first hydration shell is 180°, corresponding to a dipole moment vector oriented along the Hg−O direction. The ϕ distribution for the first shell drops to zero for bigger angles (∼ 40−45°) as compared to first transition row metal ions such as Ni^{2+} and Zn^{2+} (for which the ϕ distribution is zero already at 30°).[3] Therefore, the water molecules in the first hydration shell of the Hg^{2+} ion have a wider wagging movement than that observed in octahedral complexes. The behavior of the second shells is very similar, although it has a shallower peak, indicating less tightly oriented water molecules. At longer distances, no preferred orientations can be observed. Calculations of the ψ and ϕ angular distributions performed on the SPC/E trajectory yields almost identical results (data not shown). As it is not possible to establish whether a water molecule is rotating in its plane or is really tilted using the ϕ angle definition alone, the

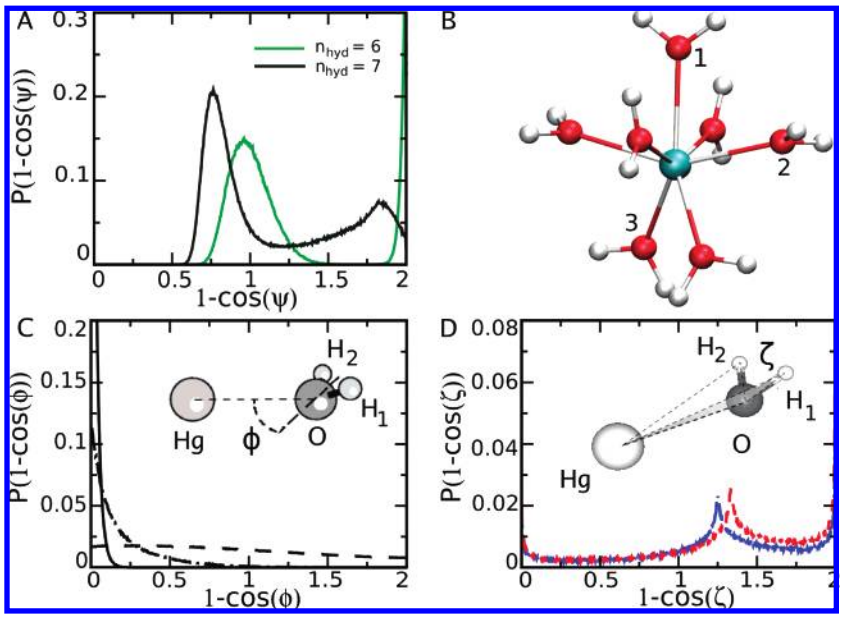

Figure 3. (A) O−Hg−O (ψ) angular distribution function for the hepta- (black line) and hexacoordinated first shell structures (green line) in the TIP5P trajectory. (B) Perspective view of the minimum energy configuration for $[Hg(H_2O)_7]^{2+}$ complex with C_2 symmetry.[13] (C) Tilt angle (ϕ) distribution functions: first hydration shell (solid line), second hydration shell (dot−dashed line), and bulk water (dashed line) in the TIP5P trajectory. (D) First-shell dihedral angle (ζ) distribution function for the SPC/E (red dashed line) and TIP5P trajectories (blue dot−dashed line).

ζ angular distribution function has been calculated (Figure 3D). The results are very similar for the two simulations and show a very sharp peak for $\zeta = 180°$, indicating that the not-tilted position is the most probable. However, a second peak is present at ~104° for the TIP5P simulation and at ~109° for the SPC/E simulation, corresponding to the A(HOH) angle of the two water models.

3.3. EXAFS Signal from MD Simulation. $\chi(k)$ theoretical signals have been calculated by means of eq 7 starting from the total SPC/E and TIP5P Hg−O and Hg−H $g(r)$'s, and the structural parameters derived from the MD simulations were kept fixed during the EXAFS analyses. In this way, the first hydration shell structure obtained from the simulations can be directly compared with experimental data, and the validity of the theoretical framework used in the simulations can be assessed. In the upper panels of Figure 4, the comparison between the EXAFS experimental signal and the theoretical curves calculated for the SPC/E and TIP5P simulations are shown. The agreement between the calculated EXAFS spectra and the experimental data is very good in both cases, proving the correctness of the structural results obtained from the two simulations. The S_0^2 value was found to be equal to 0.98, and E_0 was 12285 eV, in both cases. It is important to stress that the theoretical $\chi(k)$ signals calculated from the Hg−O and Hg−H radial distribution functions obtained from the heptacoordinated frames are identical to those calculated from the total $g(r)$'s, as the EXAFS techniques is not sensitive to the small percentage of hexacoordinated complexes. The Fourier transform (FT) modules of the EXAFS $\chi(k) \times k^2$ theoretical and experimental signals are also shown in Figure 4. The FTs have been calculated in the k-range of 2.1−13.5 $Å^{-1}$, with no phase shift correction applied. The FT spectra show a prominent first-shell peak that is mainly due to the Hg−O first-shell distance.

To gain deeper insight into the structural properties of the Hg^{2+} aqua ion, we have also calculated the EXAFS theoretical signal associated with the $g_{Hg-O}(r)$ calculated from the MD frames with a first-shell octahedral complex (Figure 1C). The results of this analysis are shown in the lower panels of Figure 4, and, in this case, the agreement between the experimental and theoretical data is not good, for both the SPC/E and TIP5P water models. The same discrepancy is found for the corresponding FTs. In this case, the S_0^2 value was found to be equal to 0.87, and E_0 was 12283 eV, for both minimizations.

3.4. Dynamical Properties. During both simulations, the Hg^{2+} ion is surrounded for most of the time by seven water molecules, and a total of 42 and 50 exchange events between the innermost and bulk water molecules are observed for the SPC/E and TIP5P simulations, respectively. The longest lifetime of the hexahydrated cluster is 1760 ps in the TIP5P simulation, vs 370 ps in the SPC/E one. Since the exchange dynamics between the six- and eight-coordinated complexes and the dominant seven-coordinated form are similar in the two simulations, two of these exchange events (corresponding to the longest lifetimes of six- and eight-coordinated complexes) have been analyzed in the case of the TIP5P simulations. Figure 5A shows the Hg−O distances in the first hydration shell around the time window corresponding to an exchange event from a heptacoordinated to a hexacoordinated cluster and back (distances are plotted up to a value of 3.2 Å, corresponding to the middle of the $g_{HgO}(r)$ depletion zone between the first and second shells). The Hg−O distance of the water molecule leaving the hydration shell is shown in a blue dot−dashed line, while the black line is the overimposition of Hg−O distances of the water molecules not taking part to the exchange event, and the red line represents the Hg−O distance of the water molecule that enters the first hydration shell after 1.76 ns. Inspection of Figure 5A clearly shows that the water molecules in the heptacoordinated complex coordinate the Hg^{2+} ion at longer distances and are less tightly bound as compared to the octahedral cluster. In Figure 5B we report the Hg−O distances when an eighth water molecule enters the first heptahydrated shell (red line) and another water molecule leaves the first shell after 40 ps (blue line). In this case, the Hg−O distance distribution grows and becomes noisier for all of the eight water molecules.

We have shown that the Hg^{2+} first-shell exchange dynamics occurs in the nanosecond time scale as a result of the relative stability of nondominant hydration species. To further describe the behavior of the dominant seven-coordinated complex, we

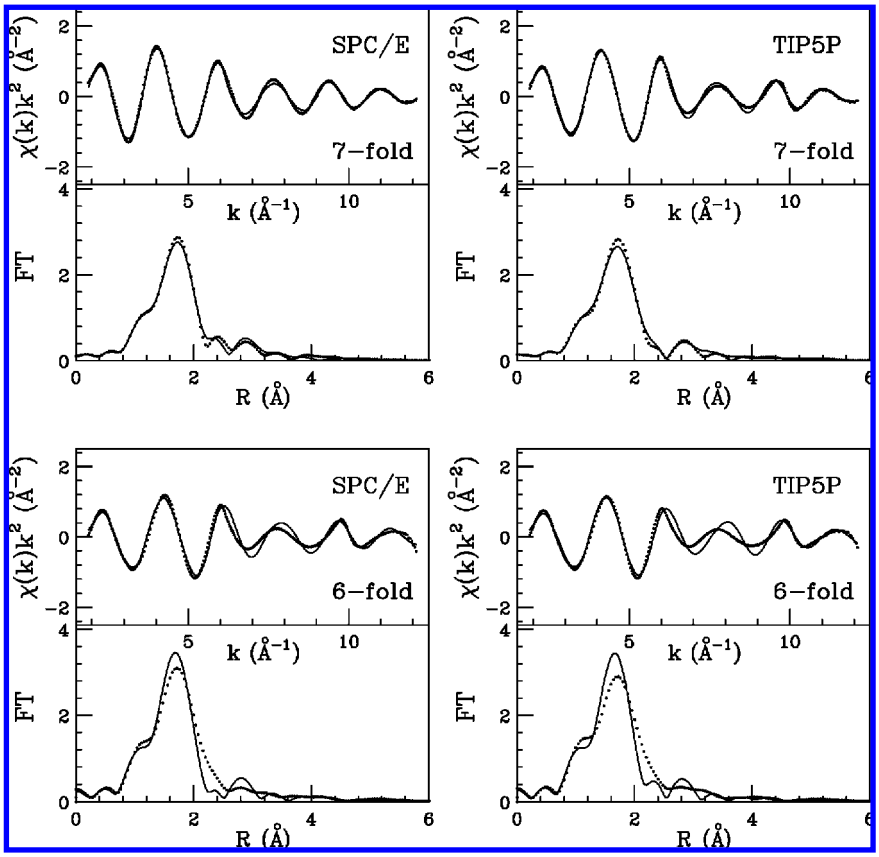

Figure 4. EXAFS theoretical signal calculated from the MD simulations (solid line) and obtained from the experiment (dotted line) for the SPC/E and TIP5P hexahydrated and heptahydrated first-shell clusters. Lower panel: FTs of the calculated (solid lines) and experimental (dotted lines) signals.

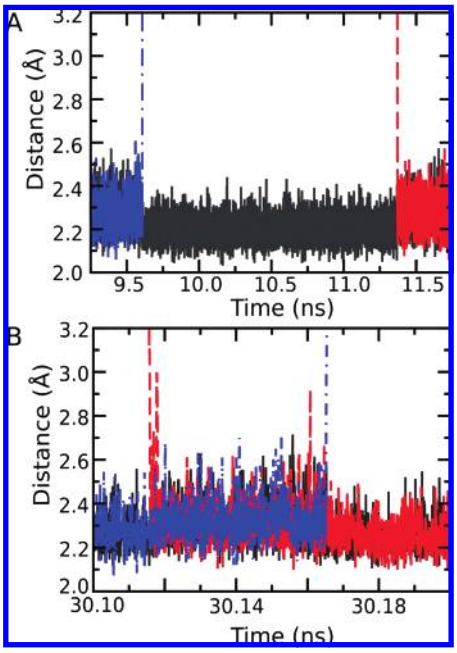

Figure 5. Hg−O distance for first shell water molecules as a function of simulation time for the TIP5P simulation. The solid black line is the average Hg−O distance of water molecules that do not participate to the exchange process, the dot-dashed blue line is the Hg−O distance of the water molecule leaving the first hydration shell, and the dashed red line is the Hg−O distance of the water molecule entering the first hydration shell. (A) The simulation window of the longest lifetime of the six-coordinated complex is shown. (B) The simulation window of the longest lifetime of the eight-coordinated complex is shown.

have calculated its diffusion coefficient D_{Hg} and reorientational correlation functions. These properties converge in the pico-second time scale, and to evaluate statistical errors, we have used five different 1000 ps time windows, equally spaced over the 58 and 57 ns of frames with a heptacoordinated first hydration shell in the SPC/E and TIP5P simulations, respectively. Since D_{Hg} strongly depends on the water−ion interactions, and consequently on the water model used, a direct comparison between different water models can be made only on properly normalized values.[32] For this reason the D_{Hg} coefficients obtained from the SPC/E and TIP5P simulations have been divided by the correspondent self-diffusion coefficients of bulk water, D_W. Similarly, the comparison with the experimental data has been performed using the D_{Hg}/D_W ratio. The calculated and experimental ion and water diffusion coefficients are shown in Table 3. Since the longest lifetime of the hexacoordinated complex in the simulation with the TIP5P water model is sufficiently long (1.76 ns), it is possible to estimate the ion diffusion coefficient even for this hydration structure. Three partially overlapping blocks of 1000 ps in the 0−1760 ps time window were used to calculate the mean square displacement. The SPC/E trajectory does not contain such a long time window with a six-coordinated first shell, and thus it is not possible to use this procedure. The ratios obtained for the

TABLE 3: Calculated and Experimental Diffusion Coefficients (10^{-5} cm^2 s^{-1}) for Hg^{2+} (D_{Hg}) and Water (D_W)

	D_{Hg}	D_W	D_{Hg}/D_W
TIP5P	1.061	2.812	0.377
TIP5P[a] ($n_{hyd} = 6$)	1.161	2.812	0.413
SPC/E	1.023	2.732	0.374
experimental[b]	0.847	2.299	0.368
experimental[b]	0.913	2.299	0.397

[a] For the TIP5P simulation, the diffusion coefficients calculated for the six-coordinated complex are also reported. [b] Reference 33.

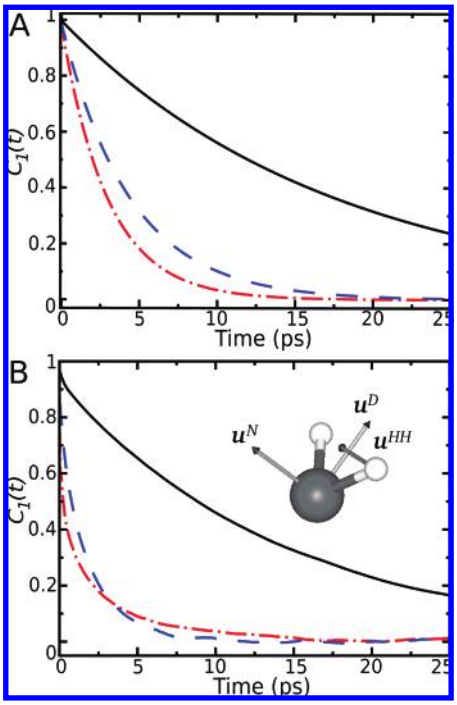

Figure 6. First-rank reorientational correlation functions $C_1(t)$ for Hg^{2+} first hydration shell: $\mathbf{u^D}$ (black solid line), $\mathbf{u^{HH}}$ (blue dashed line), and $\mathbf{u^N}$ (red dash−dotted line). The relative vectors are showed in the inset of panel B. (A) Correlation functions obtained using the SPC/E water model. (B) Correlation functions obtained using the TIP5P water model.

TABLE 4: First Reorientational Correlation Times (ps) of TIP5P and SPC/E Water Molecules in the First Hydration Shell of Hg^{2+} and in Bulk Water[a]

	vector	Hg^{2+} first shell	bulk water
TIP5P	$\mathbf{u^{HH}}$	1.6 (0.2)	4.6 (0.1)
	$\mathbf{u^D}$	12.9 (1.4)	3.7 (0.1)
	$\mathbf{u^N}$	1.6 (0.2)	2.4 (0.1)
SPC/E	$\mathbf{u^{HH}}$	2.8 (0.2)	4.1 (0.1)
	$\mathbf{u^D}$	32.7 (1.9)	4.4 (0.1)
	$\mathbf{u^N}$	2.6(0.2)	3.0 (0.1)

[a] Standard deviations are reported in parentheses.

TIP5P and SPC/E simulations (seven-coordinated frames) are very close (0.377 and 0.374, respectively) and compare well with the experimental determinations (0.368−0.397). The D_{Hg}/D_W ratio calculated from the six-coordinated frames (TIP5P water model) is 0.413, thus it is in slightly worse agreement with experimental data.

To further characterize the dynamical behavior of water molecules in the first hydration shell, we have calculated the three first-rank reorientational correlation functions, $C^{\alpha}_{l=1}$of eq 4. Figure 6A,B shows the C^{α}_1 functions for SPC/E and TIP5P first hydration shells (the selected time window has correlation times with smallest deviation from the average value), and Table 4 reports the average first shell and bulk water first rank correlation times. Both in the SPC/E and TIP5P simulations, the bulk water $\mathbf{u^N}$ vector rotates faster than $\mathbf{u^{HH}}$ and $\mathbf{u^D}$. The same result was obtained in MD simulations of pure water, showing that water rotation in the bulk is anisotropic.[25]

As far as the Hg^{2+} first hydration shell is concerned, the $\mathbf{u^D}$ correlation time is 1 order of magnitude bigger than the other two values. This finding shows that the presence of the ion strongly hinders the rotation of the hydrogen atoms toward the ion, making the rotation around the water dipole the dominant motion, in agreement with previous results.[12] On the other hand, the first hydration shell $\mathbf{u^N}$ and $\mathbf{u^{HH}}$ first-rank correlation functions go to zero slightly faster than bulk water ones, in both simulations. The two water models have a very similar behavior, and the reorientation of water molecules in the first hydration shell mainly depends on the $\mathbf{u^D}$ correlation time. Note that the reorientation of first hydration shell water molecules occurs on the picosecond time scale, that is, of the same order of magnitude of the average lifetime of the eight-coordinated complex (∼28 and ∼14 ps for SPC/E and TIP5P, respectively) while the exchange of water molecules between six- and seven-coordinated complexes occurs in the nanosecond time scale; thus the breakdown of the solvation shells involves more complicated mechanisms than simple molecular reorientations.

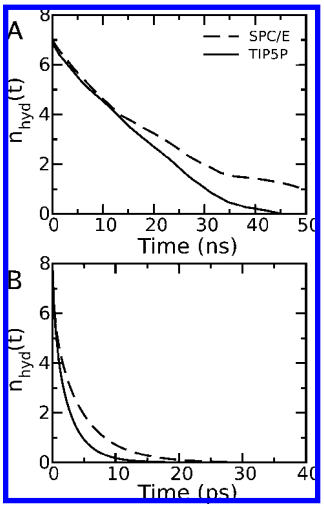

Figure 7. Time-dependent hydration numbers (or survival functions) $n_{hyd}(t)$ as obtained by application of the Impey method on the TIP5P (solid line) and SPC/E (dashed line) trajectories. (A) First hydration shell time-dependent hydration numbers. (B) Second hydration shell time-dependent hydration numbers.

TABLE 5: Mean Residence Times of Water Molecules in the First and Second Hydration Shells for Hg^{2+} Calculated Using the Impey Procedure (τ_{Im}) and the Direct Method (τ_{dir}) for the TIP5P and SPC/E Simulations

		Hg^{2+} first shell (ns)	Hg^{2+} second shell (ps)
TIP5P	τ_{Im}	6.8	2.8
	τ_{dir}	6.1	0.8
SPC/E	τ_{Im}	7.4	3.6
	τ_{dir}	7.0	1.3

Table 5 shows water mean residence times for both the first and second hydration shells obtained from the SPC/E and TIP5P simulations. In the present case we have chosen a t^* value equal to the time interval between saved configurations (25 fs), and a cutoff range to define the first hydration shell of 3.8 Å. The time-dependent coordination numbers $n_{hyd}(t)$, defined in eq 5 and used to calculate τ_{Im}, are shown in Figure 7A for the TIP5P and SPC/E simulations. Initial $n_{hyd}(0)$ values are 6.95 and 6.97 for the TIP5P and SPC/E simulations, respectively, which correspond to the average coordination numbers observed in the two simulations. The TIP5P time-dependent coordination number goes to zero after 45 ns. This means that, after this time, all the water molecules initially present in the first hydration shell have exchanged with bulk waters. In the case of the SPC/E trajectory, a water molecule remains in the first hydration shell during the whole simulation, so that the survival function does not go to zero after 60 ns. The calculated first hydration shell residence times τ_{Im} obtained by fitting $n_{ion}(t)$ to an exponential function are 7.4 and 6.8 ns for the SPC/E and TIP5P water models, respectively. Use of a "direct calculation approach"[27] gives τ_{dir} values of 7.0 and 6.1 for the SPC/E and

TIP5P simulations, respectively. The residence time of water molecules in the second hydration shell has been calculated by defining a cutoff distance in the range 3.8 and 5.5 Å, and using the same value for t^*. In this case, the survival functions go to zero after 25 ps (see Figure 7B) and the calculated τ_{Im} are 3.6 and 2.8 ps, while τ_{dir} yields results of 1.3 and 0.8 ps for TIP5P and SPC/E, respectively.

4. Discussion

We have carried out long-time MD simulations using new effective two-body interaction potentials and, for the first time, we have compared the structural results with EXAFS experimental data. The outstanding outcome is that the Hg^{2+} ion forms a stable 7-fold coordinated complex in aqueous solution, at variance with the usually accepted octahedral model reported in the literature.[1,34] In a previous QM/MM investigation, a small percentage (6.4%) of the heptacoordinated structure was found, but it was described as a transition state between two different hexacoordinated energy minima in an associative interchange mechanism.[8] The unusual hydration structure of the Hg^{2+} ion prompted us to evaluate the effect of water−water interactions on the structural and dynamic results obtained, using two different water models, namely SPC/E and TIP5P. Both simulations started from the generally accepted octahedral hydration structure for the Hg^{2+} ion, and only after a very long induction time (630 and 755 ps for the SPC/E and TIP5P water models, respectively) was the first transition to a heptacoordinated cluster observed. Thereinafter, several transitions between stable hexa- and heptacoordinated complexes have been observed during both simulations. As a consequence, a simulation time of 60 ns was necessary to properly define the first shell coordination number.

The first conclusion that can be drawn is that our approach, based on long enough classical simulations with potential not biased toward a specific first shell coordination number, is the only method able to determine the coordination geometry of a hydrated ion having a slow exchange dynamic. QM/MM or Car−Parrinello simulations, in fact, are computationally very expensive, and can model the aqueous solutions only up to a few hundred picoseconds. Therefore, these techniques are not able to reproduce exchange events occurring in the nanosecond time scale, and, in this case, they can provide useful information only if the initial configuration is the correct one.

The two water models used in the simulations provide quite similar first shell structural parameters, and these results have been compared with EXAFS experimental data. In the case of disordered systems such as ionic solution, the EXAFS technique is not able to provide unique information on the coordination number of the photoabsorber atom because of the large correlation between coordination numbers and Debye−Waller factors. However, Miyanaga et al.[35] showed that the Debye−Waller factors reflect the strength and stiffness of the ion-oxygen first-shell bond of 3d metal ions in water. In the case of the Hg^{2+} aqueous solution, the structural oscillations of the EXAFS experimental signal (see upper panels of Figure 4) decrease very rapidly, giving somehow larger Debye−Waller factors than expected for an octahedral coordination complex. Therefore, the kinetic stability of the Hg^{2+} hydration complex is lower as compared to that of 3d metal ions.

Direct comparison of the $\chi(k)$ signals calculated from the total MD $g(r)$'s results with the EXAFS experimental data allows a direct estimate of the accuracy of the Hg−O first shell distances obtained from the two simulations. As shown in the upper panels of Figure 4, the agreement between the theoretical and experimental data is very satisfactory for both the simulations, despite the small difference of the $g_{HgO}(r)$ first maxima (0.02 Å) previously described. This is not surprising, as 0.01−0.03 Å is the error associated with the EXAFS determination of first shell distances in the case of disordered systems. Conversely, the agreement between the EXAFS experimental data and the theoretical signals associated with the $g(r)$'s obtained from the hexacoordinated frames is not satisfactory for both water models (see lower panels of Figure 4). In particular, the amplitude of the theoretical signals is too strong as compared to the experimental spectrum in the k range between 6 and 10 $Å^{-1}$. This finding indicates that the octahedral hydration complexes are too rigid to reproduce the EXAFS data and, once more, proves that the Hg^{2+} first hydration shell is quite flexible. Note that the higher flexibility of the heptacoordinated hydration complex as compared to that of the octahedral cluster has been clearly highlighted by the axial−radial 2D density maps (Figure 2) and by the first-shell Hg−O distance dispersions (Figure 5A). The similarity of the results obtained from the two water models for the essential structural and dynamical properties gives further support for the heptacoordination of the Hg^{2+} ion in aqueous solution.

The structural parameters of Hg^{2+} hydration were recently investigated by means of ND with isotopic substitution.[6] This technique provides accurate information on the ion−H $g(r)$'s, while this information is not accessible from the XRD technique. Note that the knowledge of the Hg−H $g(r)$ allows one to gain deeper insight into the microscopic structure of aqueous solutions and furnish an additional check on the coordination number and the stability of the first hydration shell. The number of D atoms in the Hg^{2+} first hydration shell determined from this ND investigation is 13.5 ± 2.1, and this result is in agreement with the existence of a heptacoordinated cluster.[6] Note that the D coordination number is determined by ND with better accuracy as compared to the O coordination number, which has been found to be 5.8 ± 1.8. The Hg−O and Hg−H distances were found to be 2.48 ± 0.05 Å and 3.08 ± 0.05 Å, respectively. The Hg−O distance obtained by ND is larger by ∼ 0.1 Å than that obtained by XRD. This discrepancy has been interpreted by the authors as being due to the shift of the electronic shell of the oxygen atom toward the Hg^{2+} cation so that the X-rays scattered by electronic clouds, and neutrons scattered by atomic nuclei, find the O atoms in different positions relative to the Hg atom. However, this discrepancy can be also due to the flexibility of the first hydration shell, which gives rise to a high dispersion of the Hg−O distances that is better detected by ND.

The exchange rate constant for water molecules in the first hydration shell of Hg^{2+} has been estimated to be in the nanosecond time scale,[36] which is beyond the directly measurable scale of the current experimental techniques. In line, the mean residence times of water molecules in the first Hg^{2+} hydration shell obtained from both simulations (see Table 5) are in the nanosecond time scale. Note that the SPC/E first shell water mean residence time obtained using the Impey method is longer than all the other calculated values. This may be related to a higher sensitivity of the Impey method to the outlier behavior of a single water molecule. A previous theoretical determination of the water exchange process has been carried out from QM/MM−MD simulations using the Impey method.[9] In this work the residence time of water molecules in the first hydration was estimated to be 87 ps, but the whole simulation length was only 18 ps, and during this period, only two water exchange processes between the first and second hydration shells

were observed. Therefore, in this case application of the Impey procedure is expected to provide unreliable results.

Mean water residence times for second hydration shells are very similar to bulk water ones in both simulations (see Table 5). In this case, application of the Impey and direct methods for both simulations gives results in agreement with the experimental determinations for the mean lifetime of H-bonds in pure water,[37] indicating that water molecules in the second hydration shell have a dynamical behavior similar to that of bulk solvent.

A last remark we would like to make concerns the first shell water exchange mechanism. In a previous work, Rode and coworkers[9] proposed that the water exchange process proceeds through an associative mechanism with a seven-coordinated intermediate having a lifetime of only 1 ps, while our simulations show the existence of a dissociative mechanism where the six-coordinated complex has a much longer average lifetime (about 0.5 ns).

5. Summary

In this work, we have performed two MD simulations of the Hg^{2+} ion in aqueous solution, using a recently developed effective ion−water two body potential, and the SPC/E and TIP5P water models. Both simulations indicate the existence of a stable heptahydrated cluster for the Hg^{2+} ion, even if long induction times are needed to observe the first transition from the starting octahedral complex to the seven-coordinated one. Structural and dynamical results are very similar between the two simulations. An accurate comparison between calculated and EXAFS experimental data was made, and structural parameters on the first hydration shell were discussed in detail, providing a good agreement between the two independent approaches.

The atomic description derived from the MD simulations allowed us to determine the exchange dynamics between six-, seven-, and eight-coordinated first shell complexes, and the existence of a dissociative first shell water exchange mechanism was singled out. The mean residence time of the water molecules in the first hydration shell was also calculated, and it was found to be in the nanosecond time scale, in agreement with the experimental estimate. Moreover, additional analyses, such as ion diffusion coefficient calculations and water reorientational correlation functions were carried out, providing a detailed picture of the Hg^{2+} first hydration shell dynamics.

Acknowledgment. We gratefully acknowledge the CASPUR supercomputing consortium for providing the computational resources used in this work.

References and Notes

(1) Richens D. T. *The Chemistry of Aqua Ions*; Wiley: New York, 1997.

(2) Johansson, G.; Sandström, M. *Acta Chem. Scand., Ser. A* **1978**, *32*, 109−113.

(3) Chillemi, G.; D'Angelo, P.; Pavel, N. V.; Sanna, N.; Barone, V. *J. Am. Chem. Soc.* **2002**, *124*, 1968−1976. Chillemi, G.; Barone, V.; D'Angelo, P.; Mancini, G.; Persson, I.; Sanna, N. *J. Phys. Chem. B* **2005**, *109*, 9186−9193.

(4) Helm, L.; Merbach, A. E. *Coord. Chem. Rev.* **1999**, *187*, 151−181.

(5) Åekesson, R.; Persson, I.; Sandström, M.; Wahlgren, U. *Inorg. Chem.* **1994**, *33*, 3715−3723.

(6) Sobolev, O.; Cuello, G. J.; Román-Ross, G.; Skipper, N. T.; Charlet, L. *J. Phys. Chem. A* **2007**, *111*, 5123−5125.

(7) Babu, C. S.; Lim, C. *J. Phys. Chem. A* **2006**, *110*, 691−699.

(8) Kritayakornupong, C.; Rode, B. M. *J. Chem. Phys.* **2003**, *118*, 5065−5070.

(9) Kritayakornupong, C.; Plankensteiner, K .; Rode, B. M. *Chem. Phys. Lett.* **2003**, *371*, 438−444.

(10) Floris, F.; Persico, M.; Tani, A.; Tomasi, J. *Chem. Phys. Lett.* **1992**, *199*, 518−524.

(11) Arab, M.; Bougeard, D.; Smirnov, K. S. *Chem. Phys. Lett.* **2003**, *379*, 268−276.

(12) Egorov, A. V.; Komolkin, A. V.; Lyubartsev, A. P.; Laaksonen, A. *Theor. Chem. Acc.* **2006**, *115*, 170−176.

(13) Chillemi, G.; Mancini, G.; Sanna, N.; Barone, V.; Della Longa, S.; Benfatto, M.; Pavel, N. V.; D'Angelo, P. *J. Am. Chem. Soc.* **2007**, *129*, 5430−5436.

(14) Berendsen, H. J. C.; Grigera, J. R.; Straatsma, T. P. J. *Phys. Chem.* **1987**, *91*, 6269−6271.

(15) Mahoney, M. W.; Jorgensen, W. L. *J. Chem. Phys.* **2000**, *112*, 8910−8922.

(16) Benedict, W. S.; Gailar, N.; Plyler, E. K. *J. Chem. Phys.* **1956**, *24*, 1139−1165.

(17) Berendsen, H. J. C.; van der Spoel, D.; van Drunen, R. *Comput. Phys. Commun.* **1995**, *95*, 43−56.

(18) Berendsen, H. J. C.; Postma, J. P. M.; van Gusteren, W. F.; Di Nola, A.; Haak, J. R. *J. Comput. Phys.* **1984**, *81*, 3684−3690.

(19) Darden, T.; York, D.; Pedersen, L. J. *J. Chem. Phys.* **1993**, *98*, 10089−10092.

(20) Essmann, U.; Perera, L.; Berkowitz, M. L.; Darden, T.; Lee, H.; Pedersen, L. G. J. *J. Chem. Phys.* **1995**, *103*, 8577−8592.

(21) Hummer, G.; Pratt, L. R.; Garcia, A. E. *J. Phys. Chem. A* **1998**, *102*, 7885−7895.

(22) Allen, M. P.; Tildesley, T. J. *Computer Simulations of Liquids*; Oxford Science Publications: Oxford, 1987.

(23) van der Spoel, D.; Lindahl, E.; Hess, B.; van Buuren, A. R.; Apol, E.; Meulenhoff, P. J.; Tieleman, D. P.; Sijbers, T. M.; Feenstra, K. A.; van Drunen, R.; Berendsen, H. J. C. *Gromacs User Manual version 3.3*; www.gromacs.org, 2005.

(24) Madden, P.; Kivelson, D. *Adv. Chem. Phys.* **1994**, *56*, 467−566.

(25) van der Spoel, D.; van Mareen, P. J.; Berendsen, H. J. C. *J. Chem. Phys.* **1998**, *108*, 10220−10230.

(26) Impey, R. W.; Madden, P. A.; McDonald, I. R. *J. Phys. Chem.* **1983**, *87*, 5071−5083.

(27) Rode, B. M.; Schwenk, C. F.; Hofer, T. S.; Randolf, B. R. *Coord. Chem. Rev.* **2005**, *249*, 2993−3006.

(28) Filipponi, A.; Borowski, M.; Bowron, D. T.; Ansell, S.; Di Cicco, A.; De Panfilis, S.; Itiè, J.-P. *Rev. Sci. Instrum.* **2000**, *71*, 2422−2432.

(29) Filipponi, A.; Di Cicco, A.; Natoli, C. R. *Phys. Rev. B* **1995**, *52*, 15122−15134.

(30) Hedin, L.; Lundqvist, B. I. *J. Phys. C* **1971**, *4*, 2064−2083.

(31) Krause, M. O.; Oliver, J. H. *J. Phys. Chem. Ref. Data* **1979**, *8*, 329−338.

(32) De Araujo, A. S.; Sonoda, M. T.; Piro, O. E.; Castellano, E. E. *J. Phys. Chem. B* **2007**, *111*, 2219−2224.

(33) Lide, D. R. *CRC Handbook of Physics and Chemistry*, 84th ed.; CRC Press: Boca Raton, FL, 2003.

(34) Othaki, H.; Radnai, T. *Chem. Rev.* **1993**, *93*, 1157−1204.

(35) Miyanaga, T.; Sakane, H.; Watanabe, I. *Bull. Chem. Soc. Jpn.* **1995**, *68*, 819−824.

(36) Eigen, M. *Pure Appl. Chem.* **1963**, *6*, 97−115.

(37) Lock, A. J; Woutersen, S.; Bakker H. J. *Femtochemistry and Femtobiology*; World Scientific Publishing: Singapore, 2001.